

# COMPARISON OF FATIGUE CRACK GROWTH CONCEPTS WITH RESPECT TO INTERACTION EFFECTS

M. Sander

University of Paderborn, Institute of Applied Mechanics  
Pohlweg 47-49, D-33098 Paderborn, Germany  
sander@fam.upb.de

## Abstract

Within the scope of this paper the results of lifetime prediction concepts are presented with respect to interaction effects in comparison to appropriate experimental data of the aluminium alloy 7075 T651. Therefore following loading situations are used: overloads, overload sequences and block loadings with different load ratios as well as service loadings in terms of three standard load sequences CARLOS vertical, FELIX/28 and WISPER. It can be shown that the lifetime depends both on the used concept and on the loading sequence. Also the influence of the parameters, which must be fitted by experimental data for all analytical prediction models, has been investigated.

## Introduction

Against the background of damage-tolerant dimensioning of structures and components in particular in the aerospace industry, but also in other sectors of industry like the reactor technique or the shipbuilding, a reliable computed lifetime prediction is of great importance. Due to existing interaction effects during the fatigue crack growth under variable amplitude loading this lifetime prediction is very complex. In the last 20 years several prediction models have been developed. All of them base on different explanations of the interaction effects, which affect the prediction. The lifetime prediction of components or structures must be conservative for safety-engineering reasons independent of the material or the load spectrum. For economical reasons the safety-factor should not exceed a certain value e.g. in order to utilise the material optimally or to allow a light weight construction. Whether a lifetime prediction leads to acceptable results, admittedly depends on the reliability of the prediction concept. Therefore it is necessary to verify the results of the concepts by means of appropriate experimental data of service load spectra.

## Models for predicting the crack growth under variable amplitude loading

The concepts for predicting the crack growth and the lifetime under variable amplitude loading can be divided into global and cycle-by-cycle analyses (Fig. 1). The global models try to predict the fatigue crack growth by the consideration of the whole loading cycles together. Whereas the concepts with a cycle-by-cycle-analysis evaluate each cycle separately and by an accumulation of the separate analyses the overall analysis is built. A cycle-by-cycle analysis can be performed on the one hand with and on the other hand without taking interaction effects into account. Schijve [1] divided the models, which consider the interaction effects, into three main categories: the yield zone models, crack closure models and the strip yield models.

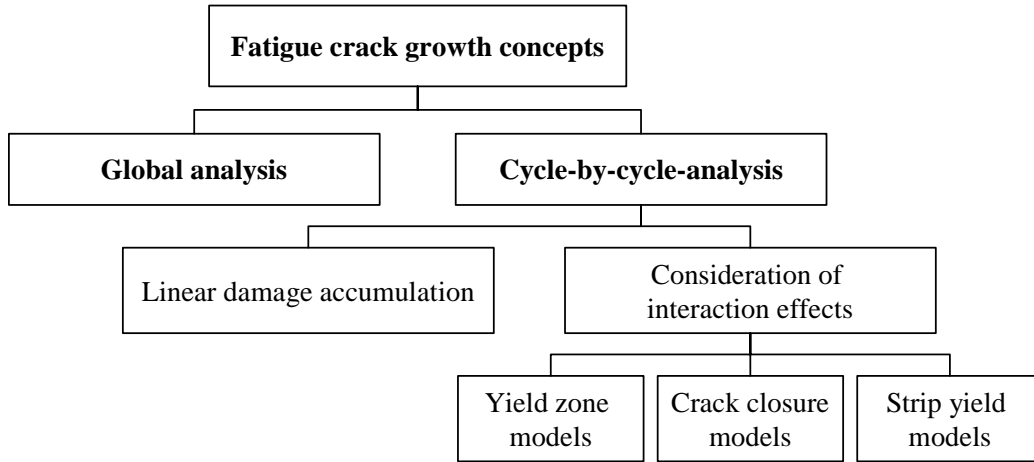


FIGURE 1. Classification of fatigue crack growth concepts.

### *Global analyses models*

The global analyses models base on the statistical description of the load spectrum. The aim of these models is to calculate only one cyclic stress intensity factor from the whole load spectrum, which can be used in order to characterize the crack growth adequately. I.e. the application of this single mean value of the cyclic stress intensity factor leads to the same mean crack growth rate as the use of the load spectrum with variable amplitudes. One of the first approaches was developed by Barsom [2]. In this model a mean value

$$\Delta K_{rms} = \sqrt{\frac{1}{N} \sum_{i=1}^N \Delta K_i^2} \quad (1)$$

is calculated, which can be inserted into a crack growth equation. The global analysis models deliver only acceptable results, if the load sequence is uniformly stochastic distributed [3].

### *Linear damage accumulation*

The linear damage accumulation is set up on the functional description of the crack growth curve, whereby a cycle-by-cycle-analysis is considered. For every cycle a crack growth increment  $\Delta a_i$  is calculated separately by integration and cumulated in order to obtain a prediction for the whole load spectrum:

$$a = a_0 + \sum_{i=1}^N f(\Delta K, R, \dots) = a_0 + \sum_{i=1}^N \Delta a_i \quad (2)$$

The occurring interaction effects are not considered, wherefore this model is also called non interaction concept.

### *Yield zone models*

In the category of the yield zone models all approaches are combined, which try to explain the interaction effects by the conditions in front of the crack tip. One concept of this group is the Willenborg model [4]. Withal Willenborg assumes that by the application of an overload residual stresses  $\sigma_{ES}$  occur, which depend on the current loading and the crack growth within

the plastic zone of the overload. For the consideration of the residual stresses a virtual stress intensity factor

$$K_{max,req} = K_{max}^{ol} \sqrt{1 - \frac{\Delta a}{\omega_{ol}}} \quad (3)$$

is used, which is necessary in order to create a plastic zone of the size

$$\omega_p = \frac{\pi}{8} \left( \frac{K_{max,req}}{\alpha \sigma_{YS}} \right)^2, \quad (4)$$

that reaches the boundary of the plastic zone  $\omega_{ol}$  created by the overload (Fig. 2). Thereby the constraint factor  $\alpha$  ranges between 1.15 for plane stress and 2.55 for plane strain.

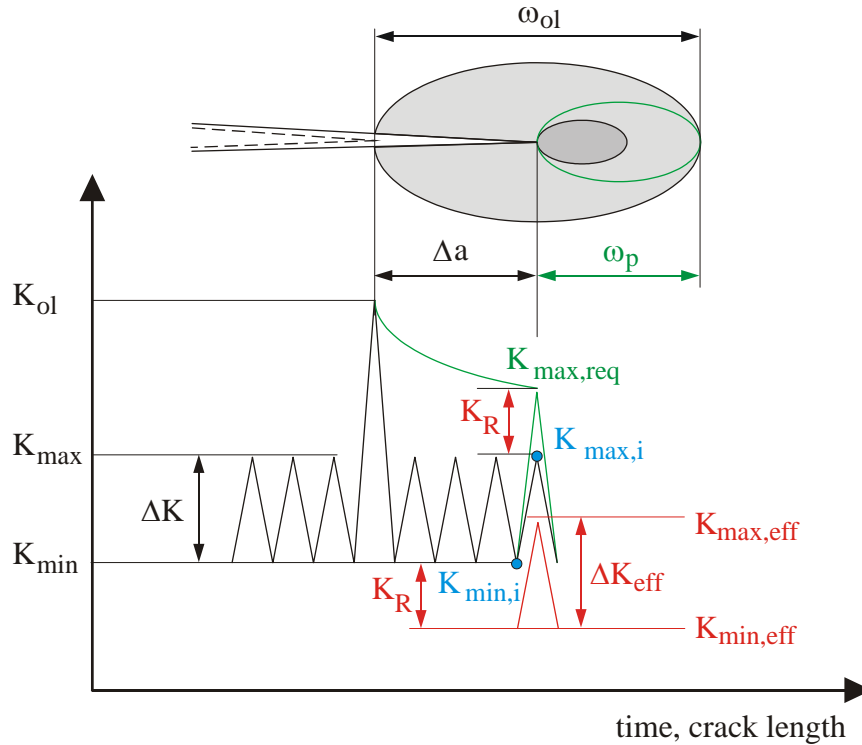


FIGURE 2. Determination of the effective stress intensity factor by the Willenborg model.

The difference between the virtual stress intensity factor  $K_{max,req}$  and the current maximum stress intensity factor  $K_{max,i}$  of a following cycle  $i$  is defined as residual stress intensity factor  $K_R$ . The retardation effect is acquired by the reduction of the stress intensity factors  $K_{max,i}$  and  $K_{min,i}$  about  $K_R$  and results in the effective cyclic stress intensity factor

$$\Delta K_{eff,i} = \begin{cases} \Delta K_i & \text{for } K_{max,eff,i} > 0 \text{ and } K_{min,eff,i} > 0 \\ K_{max,eff,i} & \text{for } K_{min,eff,i} \leq 0 \\ 0 & \text{for } K_{max,eff,i} \leq 0 \end{cases} \quad (5)$$

and the effective R-ratio

$$R_{eff,i} = \frac{K_{min,eff,i}}{K_{max,eff,i}}. \quad (6)$$

The retardation effect is annihilated when the current plastic zone (dark grey) reaches the boundary of the overload plastic zone (light grey). A disadvantage of this model is that already at an overload ratio  $R_{ol}=K_{ol}/K_{max} = 2$  crack arrest is predicted. Due to this fact this model is generalized by Gallagher [5] and implemented in NASGRO. In the generalized Willenborg model the stress intensity factor  $K_R$  is multiplied by a factor

$$\phi = \frac{1 - \frac{\Delta K_{th}}{\Delta K}}{(R_{SO} - 1)} \quad (7)$$

so that the real shut-off-ratio  $R_{SO}$  as well as the ratio of the threshold value  $\Delta K_{th}$  and the cyclic stress intensity factor  $\Delta K$  is taken into account.

In order to consider the reduction of retardation effects due to underloads the modified generalized Willenborg model is developed by Brussat and implemented in the NASGRO code [5]. The factor  $\phi$  is now given by

$$\phi = \begin{cases} 2.523\phi_0 / [1.0 + 3.5(0.25 - R_{ul})^{0.6}] & R_{ul} = K_{ul} / K_{ol} < 0.25 \\ 1.0, & R_{ul} = K_{ul} / K_{ol} > 0.25 \end{cases} \quad (8)$$

whereby  $\phi_0$  is the value of  $\phi$  for  $R_{ul}=0$  and  $K_{ul}$  the underload stress intensity factor.

### ***Crack closure models***

On the basis of the findings of Elber [6] concerning the plasticity induced crack closure the crack closure models are developed. The most known concepts are the PREFAS-model [7, 8], the ONERA-model [8, 9] and the CORPUS-model [8, 10]. In these models the crack opening stress intensity factor  $K_{op}$ , at which the crack is fully opened during a load cycle, is determined analytically cycle-by-cycle. This results in the effective stress intensity factor

$$\Delta K_{eff} = K_{max} - K_{op} \quad (9)$$

In NASGRO a constant closure model developed by Northrop [5] is implemented. It is a simplified closure model based on the observation that for some load sequences a stabilized  $K_{op}$  value can be determined, which is reflected in a crack closure factor [5].

### ***Strip Yield models***

The strip yield models are based on the assumption that the interaction effects are caused by plastically deformed material along the crack wake of a growing crack. This leads to crack closure and a reduced stress intensity factor  $\Delta K_{eff}$  (Eq. 5). In contrast to the crack closure models, the strip yield models determine  $K_{op}$  by numerical simulations with bar elements within a thin strip along the crack line. These bar elements in the plastic zone ahead of the crack tip are intact and can carry both tensile and compressive stresses, while the elements in the crack wake are broken and can only carry compressive stresses in the contact situation [5]. Outside of the strip the material is perfectly elastic. During the simulation at minimum load contact stresses are computed for elements, which due to the recent plastic deformation at maximum load are in contact. The most familiar strip yield models are developed by Newman [11] and de Koning [12]. The main difference between these two models is the definition of the constraint factor. Newman assume that the state of stress depends on the crack growth rate. At low crack velocities plain strain and at high rates plane stress is taken

for granted. The value for the constraint factor is calculated accordingly to the crack growth rate, but is constant along the elements of the plastic zone. In contrast to Newman de Koning defines the constraint factor under tension as a parabolic function along these elements, whereby at the end of the plastic zone the value of the plane stress is assumed.

## Evaluation of simulation results with experimental data

For the investigations the aluminium alloy 7075-T651 by means of CT specimen with  $w = 72$  mm and  $t = 10$  mm, which have been taken from a plate in T-L direction, is used. Because in the material database NASMAT of the program NASGRO [5] this type of aluminium in T-L direction is not available at first a fit of the necessary Forman/Mettu equation parameters [Table 1] by experimental data has been carried out. The Forman/Mettu equation [13] also called NASGRO equation is given by

$$\frac{da}{dN} = C \left[ \left( \frac{1-\gamma}{1-R} \right) \Delta K \right]^n \frac{[1 - (\Delta K_{th} / \Delta K)]^p}{[1 - (K_{max} / K_C)]^q}. \quad (10)$$

TABLE 1. Forman/Mettu equation parameters for 7075 T651.

	C	n	p	q	$\Delta K_0$ [N/mm <sup>3/2</sup> ]	$K_C$ [N/mm <sup>3/2</sup> ]
NASGRO database	$2.12 \cdot 10^{-11}$	2.885	0.5	1.0	104.25	972.28
Data fit	$2.12 \cdot 10^{-11}$	2.885	0.8	0.4	104.25	1010.8

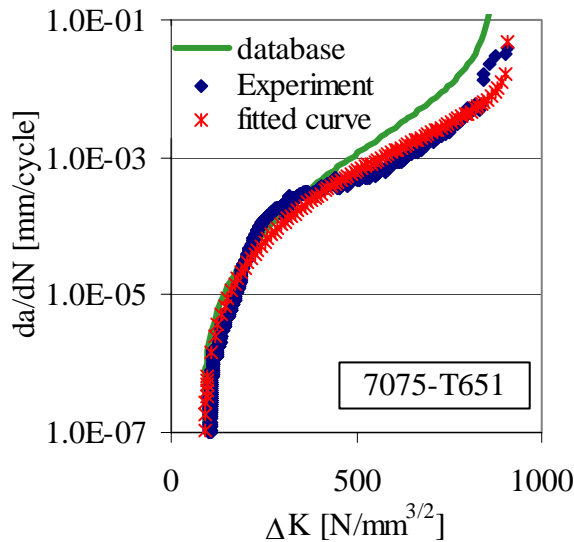


FIGURE 3. Crack growth curve for  $R = 0.1$  compared to fitted curves.

In Fig. 3 the fitted curve and the curve using the database parameters for 7075-T651 L-T compared to experimental data for  $R = 0.1$  are shown. It becomes obvious that due to the typical double S-shape of the crack growth curve the fitted curve in some regions is located beneath and in others above the experimental curve.

The simulations of fatigue crack growth under variable amplitude are performed with the program NASGRO and the therein implemented concepts. In order to validate the results also appropriate experiments are carried out. For both the simulations and the experiments following load sequences are used: overloads and block loadings with different load ratios as well as service loadings in terms of the three standard load sequences CARLOS vertical, FELIX/28 and WISPER.

For most prediction models more or less parameters must be fitted by experimental data. Fig 4 e.g. shows the influence of the user-defined closure factor of the constant closure model of

Northrop. Under constant amplitude loading with  $F_{max} = 4.5$  kN and  $R = 0.1$  as well as for single overload with an overload ratio  $R_{ol} = 2.2$ , which are interspersed into the constant amplitude loading, the best results are obtained with a closure factor of 0.2, while for the load spectra WISPER and FELIX/28 a factor of 0.5 seems best. With an increasing closure factor also the number of predicted cycles increase, which lead in the case of constant amplitude loadings and overloads beginning from a value of 0.3 to non-conservative results. The influence of the closure factor for the investigated load sequences is noticeable smaller, but for any closure factor bigger than 0.7 also non-conservative predictions are given.

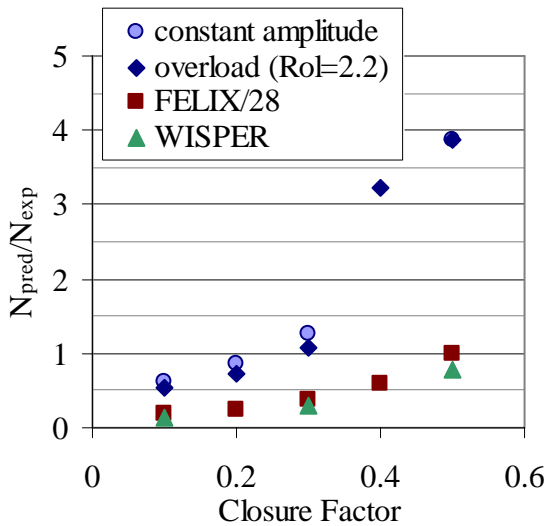


FIGURE 4. Influence of the closure factor at load spectra with variable amplitude.

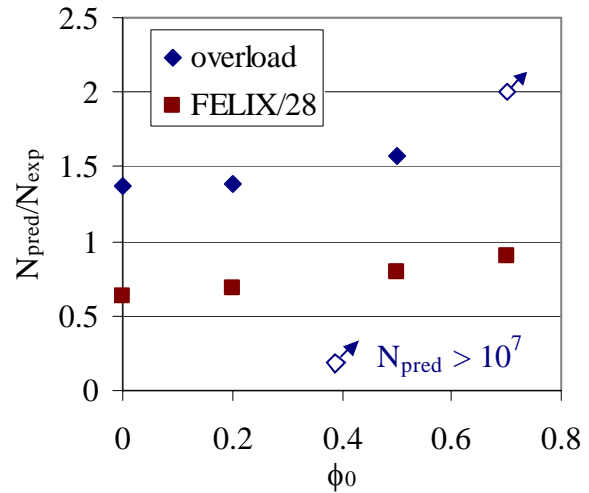


FIGURE 5. Influence of the factor  $\phi_0$ .

The shut-off-ratio  $R_{SO}$  (Eqn. 7) of the generalized Willenborg model only has a small influence on the simulation results, if the overload ratio of the loading does not exceed this limit. The shut-off-ratio of this material is assumed at 3.0. If  $R_{SO}$  is varied from 2.5 to 3.5 e.g. in the simulations with FELIX/28 only 3% differences, in other simulation also smaller differences can be observed.

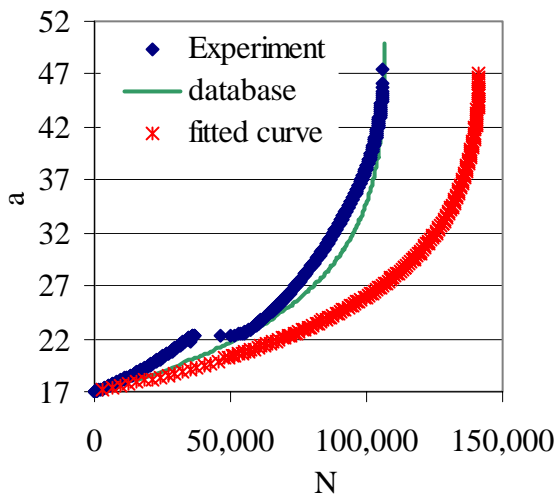


FIGURE 6. Comparison of an overload simulation with appropriate experiments.

Fig. 5 shows the influence of the factor  $\phi_0$  of the modified generalized Willenborg model (Eqn. 8). It becomes apparent that an increasing value of  $\phi_0$  also causes an increasing lifetime. It is remarkable that the simulations of the overload experiment always lead to non-conservative results independent of the factor  $\phi_0$ , while the simulation of FELIX/28 yield good results.

The reason why the simulations without taking interaction effects into account are non-conservative is shown in Fig. 6. Due to the fitting of the crack growth equation parameters the crack velocity at the beginning was underestimated for this baseline level loading, which in turn produce

this result, although a retardation occurs. For other baseline level loadings the lifetime prediction results are conservative. Fig. 6 displays in addition the same simulation, but with the equation parameters of the NASGRO database. The lifetime prediction is nearly perfect, but also at first the crack growth rate is underestimated and then due to the fitting an acceleration occurs. In other cases contrary results are observed.

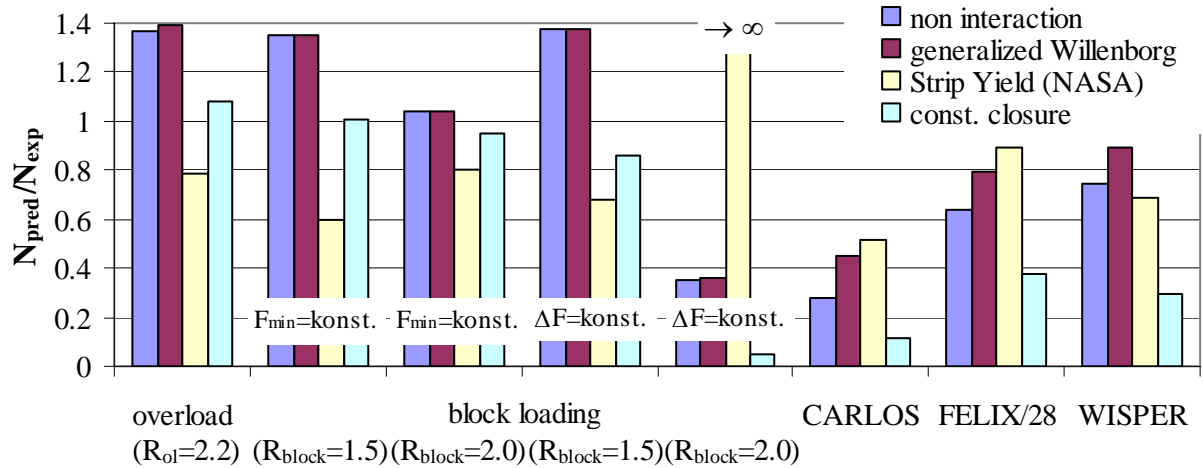


FIGURE 7. Simulations with fitted material properties compared with Experiments.

Further simulation results are illustrated in Fig. 7, where an overview of simulation results of different analytical concepts compared to experimental data for different loading situations is given. It can be seen that the simulations without the consideration of interaction effects and with the generalized Willenborg model ( $R_{SO} = 3.0$ ) for overloads ( $F_{Bl,max} = 4,5$  kN,  $R_{Bl} = 0.1$ ) and block loadings, which are interspersed into a constant baseline level loading of  $F_{Bl,max} = 5$  kN and  $R_{Bl} = 0.1$ , lead nearly to the same results, but except the block loading with  $\Delta F = 4,5$  kN =const. and  $R_{block} = 2.0$ , generate non-conservative results for the same reason as mentioned before. In contrast the Strip Yield model with a constant constraint loss option (NASA) yield conservative results for the mentioned cases. Admittedly all the simulations with the Strip Yield model are performed with the  $\Delta K_{eff}$  values of the material 7075 T6 from the material database. The simulations with the load spectra cause conservative results, whereby the best predictions are obtained with the Strip Yield model. The comparison of the load spectra shows also that the reliability of the models are affected by the load sequence. Independent from the used concept the results are overall more conservative for CARLOS than for FELIX/28 or WISPER. CARLOS is rather a stochastically distributed spectrum, while FELIX/28 and WISPER contain overloads and block loadings. The constant closure model only leads to reliable results for more or less constant loading situations.

Although good results are achieved with the generalized Willenborg model, the fundamental idea can be disproved by experimental results. From overload experiments influenced crack length increments  $\Delta a_{inf,D}$  can be determined, which describe exactly the region, in which the crack velocity is retarded. Under the assumption of the physical correctness of the yield zone concepts the calculated plastic zone size must be equal to the influenced crack length. But the experimental results show that independent of the overload ratio or the underlying equation for the calculation of the plastic zone size,  $\Delta a_{inf,D}$  is always bigger than the plastic zone size. However the results are often good, which is achieved by an appropriate fitting of the data. But besides an adaptation of the parameters on the material

also an adaptation on the load spectrum is necessary so that there is no transferability to other spectra or arbitrary components and structures [3].

But only a comparison of the predicted and experimental determined lifetimes is not sufficient enough to assess the reliability of concepts, because a good agreement between the predicted cycles and the cycles of the experiment can result from different predicted crack growth rates. For instance an initial overestimation of the crack velocity can be compensated by a slower crack growth during the further crack growth. In [14] some examples are given, which demonstrate this effect.

## Conclusions

From the simulations and the appropriate experiments it can be concluded that the concepts lead to conservative results in the cases of real service load spectra. The prediction of overload and block loading situations is not very reliable, because both conservative and non-conservative results can be obtained. For the reliability of prediction results it is necessary to attend for a good fitting of the crack growth equation.

## References

1. Schijve, J., *ASM Handbook. Fatigue and Fracture*, vol. **19**, 110-133, 1997
2. Barsom, J.M., In *Fatigue crack growth under spectrum loads*, edited by R.P. Wie, R.I. Stephens, ASTM STP 595, Philadelphia, 1976, 217-235
3. Sander, M., *Influence of variable amplitude loading on the fatigue crack growth in components or structures*, VDI-Verlag, 2003, in german
4. Dominguez, J., In *Handbook of fatigue Crack Propagation in Metallic Structures* edited by A. Carpinteri, 1994, 955-997
5. NASA, *Fatigue crack growth computer program "NASGRO", Version 3.0 – Reference manual*, 2000
6. Elber, W., *Engineering Fracture Mechanics*, vol. **2**, 37-45, 1970
7. Aliaga, D., Davy, A., Schaff, H., *Mechanics of Fatigue Crack Closure* edited by J.C. Newman Jr., 1987, 491-504
8. Padmadinata, U.H., *Investigation of crack-closure prediction models for fatigue in aluminium alloy sheet under flight-simulation loading*, PhD-thesis, Delft, 1990
9. Baudin, G., Labourdette, R., Robert, M., In *Fatigue crack growth under variable amplitude loading* edited by J. Petit, et al., Elsevier Applied Science, London, 1988, 292-308
10. de Koning, A.U., In *ASTM STP 743* edited by R. Roberts, ASTM, 1981, 63-85
11. Newman Jr., J.C., In *ASTM STP 748* edited by J.B. Chang, C.M. Hudson, 1981, 53-84
12. de Koning, A.U., van der Linden, H.H., *Prediction of fatigue crack growth rates under variable loading using a simple crack closure model* NLR MP 81023U, Amsterdam, 1981
13. Forman, R.G., Mettu, S.R., In *ASTM STP 1131* edited by Ernst, H.A. et al., 1992, 519-546



14. Sander, M., Richard, H.A., *Int. Journal of Fatigue*, vol. 25, 999-1005, 2003